

CONFIDENTIAL

356
Copy
RM L55G14

NACA

FILE
COPY

RESEARCH MEMORANDUM

FREE-FLIGHT INVESTIGATION TO OBTAIN DRAG-AT-LIFT
AND STABILITY DATA FOR A 60° DELTA-WING—BODY
CONFIGURATION OVER A MACH NUMBER
RANGE OF 1.3 TO 1.6

By Clement J. Welsh

Langley Aeronautical Laboratory
Langley Field, Va.

CLASSIFIED DOCUMENT

This material contains information affecting the National Defense of the United States within the meaning of the espionage laws, Title 18, U.S.C., Secs. 793 and 794, the transmission or revelation of which in any manner to an unauthorized person is prohibited by law.

CLASSIFICATION CHANGED TO UNCLASSIFIED
AUTHORITY: NACA RESEARCH ABSTRACT NO. 129
EFFECTIVE DATE: JULY 17, 1958
WHL

NATIONAL ADVISORY COMMITTEE
FOR AERONAUTICS

WASHINGTON

October 6, 1955

CONFIDENTIAL

NATIONAL ADVISORY COMMITTEE FOR AERONAUTICS

RESEARCH MEMORANDUM

FREE-FLIGHT INVESTIGATION TO OBTAIN DRAG-AT-LIFT
AND STABILITY DATA FOR A 60° DELTA-WING-BODY
CONFIGURATION OVER A MACH NUMBER
RANGE OF 1.3 TO 1.6

By Clement J. Welsh

SUMMARY

Flight tests have been made of a rocket-propelled 60° delta-wing-body configuration; the wing airfoil section was NACA 0003-63. Drag at lift and stability data were obtained for a Mach number range of 1.28 to 1.6.

The drag due to lift parameter increased from 0.31 to 0.38 with increasing Mach numbers, and only a small amount of leading-edge suction was obtained. Values of lift coefficient and pitching-moment coefficient varied linearly with angle of attack, and the aerodynamic-center position was nearly constant at approximately 46 percent of the mean aerodynamic chord. The damping-in-pitch derivatives varied from -1.6 to -1.2 with increasing Mach numbers. Aeroelasticity effects calculated for the tested configuration increased with increasing Mach numbers and indicated a loss in lift of about 15 percent and a forward movement of the aerodynamic center of approximately 4 percent of the mean aerodynamic chord at a Mach number of 1.6.

INTRODUCTION

As part of the National Advisory Committee for Aeronautics drag-due-to-lift program (see ref. 1, for example) a free-flight test has been made to furnish additional data for thin wings at high Reynolds numbers. A 60° delta-wing configuration having an NACA 0003-63 airfoil section was flight tested and data obtained at Reynolds numbers around 15×10^6 .

CONFIDENTIAL

Also obtained and presented in this paper are zero-lift drag, lift, and stability data, including aeroelasticity corrections. The rocket-propelled-model configuration was tested at the Langley Pilotless Aircraft Research Station, Wallops Island, Va.

SYMBOLS

M	Mach number
q	dynamic pressure
R	Reynolds number
I_y	moment of inertia about the lateral axis
S	total wing area
b	wing span
c	local chord
\bar{c}	mean aerodynamic chord
L	total lift
D	total drag
M	pitching moment
C_L	lift coefficient, L/qS
C_D	drag coefficient, D/qS
C_m	pitching-moment coefficient (relative to the center of gravity), $M/qS\bar{c}$
C_l	section lift coefficient
$C_{L_{opt}}$	optimum lift coefficient, corresponding to $(L/D)_{max}$
C_{D0}	zero-lift drag coefficient
$\frac{dC_D}{dC_L^2}$ or K	drag due to lift parameter

C_{L_α} lift-curve slope

C_{m_α} pitching-moment curve slope

$(C_{m_q} + C_{m\dot{\alpha}})$ damping-in-pitch derivatives, $\frac{\partial C_m}{\partial(\frac{\dot{\theta}\bar{c}}{2V})} + \frac{\partial C_m}{\partial(\frac{\dot{\alpha}\bar{c}}{2V})}$

y lateral distance from fuselage center line

$$\eta = \frac{y}{b/2}$$

θ pitching angle or local wing twist, in radians

α angle of attack, deg

$$\dot{\alpha} = \frac{1}{57.3} \frac{d\alpha}{dt}$$

$$\dot{\theta} = d\theta/dt$$

Subscripts:

r rigid-wing conditions

CP spanwise center of pressure

f flexible-wing conditions

s condition of full leading-edge suction

$n-s$ condition of zero leading-edge suction

MODEL AND TESTS

A sketch of the model configuration is shown in figure 1, and a photograph in figure 2.

The 60° delta wing had an NACA 0003-63 airfoil section and was constructed of solid dural; the parabolic-profile fuselage was of wood-metal construction. The fuselage ordinates are listed in table I.

The model was equipped with a telemeter which transmitted measurements including angle of attack, free-stream total pressure, and normal, longitudinal, and transverse accelerations.

Pulse rockets were installed in the rear portion of the fuselage to produce disturbances of the model in pitch about its lateral axis during flight in order that drag due to lift and stability data could be obtained.

Preflight Measurements

Experimental structural influence coefficients were obtained for the 60° delta wing corresponding to a loading along the 46-percent chord line. The coefficients which were used in the aeroelasticity corrections are listed in the following table as θ_{ij} values corresponding to the local wing twist at station (i) due to a unit load at station (j). For simplicity in listing these values, (i) and (j) are given integer values 1, 2, 3, 4, and 5 corresponding to actual spanwise stations (in inches) 4.40, 6.88, 9.10, 11.35, and 14.48. The maximum body radius is 3.25 inches and the actual semispan with the tip radius as shown in figure 1 is 16.73 inches. The values of θ_{ij} (rad per lb) as listed are (-10^6) times the true values:

θ_{11}	1.0	θ_{24}	8.0	θ_{42}	2.5
θ_{12}	1.5	θ_{25}	14.5	θ_{43}	5.0
θ_{13}	2.0	θ_{31}	1.0	θ_{44}	24.5
θ_{14}	3.0	θ_{32}	2.5	θ_{45}	102.0
θ_{15}	4.0	θ_{33}	4.0	θ_{51}	1.0
θ_{21}	1.0	θ_{34}	16.5	θ_{52}	2.5
θ_{22}	2.5	θ_{35}	44.0	θ_{53}	5.0
θ_{23}	4.0	θ_{41}	1.0	θ_{54}	24.5
				θ_{55}	240.0

Flight Test

During flight, the model was tracked with an NACA modified SCR-584 radar unit to obtain position-time data and with a Doppler radar unit to obtain velocity-time data. Atmospheric conditions were determined from radiosonde equipment. The variations of wind direction and speed with altitude were obtained by tracking the ascending radiosonde with Rawin equipment. The variations of Reynolds number and dynamic pressure of the test with Mach number are shown in figure 3.

Accuracy

Experience has indicated that the errors in the absolute value of a measured telemeter quantity are within ± 1 percent of the range of the instrument; hence, at $M = 1.45$, the errors in the normal and chordwise force coefficients have been calculated to be within ± 0.003 and ± 0.001 , respectively. Errors in Mach number and Δa are believed to be within ± 0.01 and ± 0.100 , respectively, throughout the test range.

Analysis

The disturbances in pitch resulting from the pulse rockets resulted in a maximum angle of attack of about $\pm 6^\circ$. As there were no appreciable transverse accelerations during flight, the short-period oscillations resulting from these disturbances have been analyzed assuming two degrees of freedom by the methods of reference 2. In addition, the instantaneous pitching-moment coefficients have been calculated from the two normal accelerometers as indicated in reference 3.

Expressions for $C_{L_{opt}}$ and $(L/D)_{max}$, $C_{L_{opt}} = \sqrt{\frac{C_{D_0}}{K}}$, $(\frac{L}{D})_{max} = \frac{1}{2} \sqrt{\frac{1}{KC_{D_0}}}$ are obtained from the general expression for drag coefficient, $C_D = C_{D_0} + KC_L^2$. The upper range of the C_L test data was in the range of $C_{L_{opt}}$, hence the parabolic variation of C_D against C_L was well defined.

To indicate the aeroelasticity effects on the lift and static longitudinal stability resulting from the flexibility of the 3-percent-thick solid dural wing, a brief aeroelasticity analysis was made. The method used is indicated in the appendix and makes use of wing structural influence coefficients combined with a spanwise loading for the rigid wing. As previously stated, the influence coefficients were obtained experimentally, while the spanwise loading used was that for a 68° delta wing at $M = 1.6$ (experimental curve from unpublished data). The difference in loading between the 60° and the 68° delta was assumed negligible.

DISCUSSION

The data in general are presented for a wing-body configuration having a wing with flexibility characteristics that could be representative of that of a typical missile or aircraft in this speed range.

In specific cases, curves are shown which have been corrected for aeroelasticity to indicate the range of losses in lift and static longitudinal stability that could exist on similar configurations relative to a rigid-wing condition. A plot of the flexibility parameter, effective-lift ratio, for the configuration is shown in figure 4(a).

To confirm that the assumptions made in applying the method for aeroelasticity corrections indicated in the appendix to the delta-wing configuration of the present test were justified, C_{L_a} values of the present test corrected to rigid-wing conditions and two similar configurations (ref. 4) are shown in figure 4(b). The two configurations from reference 4 furnish a good comparison being delta-wing-body configurations having wings with identical sections to that of the present test and mounted on similar bodies. As the wings were constructed of solid steel, they are assumed to be representative of nearly rigid wings.

Drag

In figure 5 typical plots of C_D against C_L and C_D against C_L^2 are shown, including test points, to give an indication of the scatter of the actual data points.

In figures 6(a) and 6(b), zero-lift drag and drag due to lift are shown against Mach number. The values of $\frac{dC_D}{dC_L^2}$ increased from 0.31 at $M = 1.28$ to 0.38 at $M = 1.6$. Shown for comparison is a calculated curve of $\left(\frac{dC_D}{dC_L^2}\right)_{n-s}$ (no leading-edge suction for the flexible wing con-

figuration). The $\left(\frac{dC_D}{dC_L^2}\right)_{n-s}$ values were calculated from the integrated effect over the wing resulting from the assumption that the resultant section force was normal to its local chord and in consideration of the spanwise varying α resulting from the flexibility of the wing. Also shown

is a $\left(\frac{dC_D}{dC_L^2}\right)_s$ curve, representative of a condition of full leading-edge suction. The $\left(\frac{dC_D}{dC_L^2}\right)_s$ curve was obtained by subtracting $\Delta \frac{dC_D}{dC_L^2}$ values

(the increment of the calculated leading-edge contribution to the $\frac{dC_D}{dC_L^2}$

of an isolated 60° delta wing when full leading-edge suction exists, ref. 5) from $\left(\frac{dC_D}{dC_L^2}\right)_{n-s}$ values.

As would be expected and as is apparent from these curves, the experimental curve of $\frac{dC_D}{dC_L^2}$ for the configuration includes a combined effect of leading-edge suction and aeroelasticity, and indicated that only a small amount of leading-edge suction was obtained. The curves also indicate the major effect that leading-edge suction can have on the drag at lift of a 60° delta wing over this speed range.

To give an indication of the performance characteristics of the configuration, $(L/D)_{max}$ and C_{Lopt} have been plotted against Mach number in figures 7(a) and 7(b). $(L/D)_{max}$ decreased from 6.6 to 5.8 with increasing Mach number; C_{Lopt} remained nearly constant over the test range at approximately 0.24.

Stability

Both C_L and C_m values varied linearly with α throughout the test range and their corresponding slopes are plotted in figures 8(a) and 8(b) against Mach number; both $C_{L\alpha}$ and $C_{m\alpha}$ decreased with increasing Mach number. Also shown are $C_{L\alpha}$ and $C_{m\alpha}$ curves corrected for aeroelasticity.

As is obvious, the aeroelasticity effects increased with increasing Mach numbers, and at $M = 1.6$ the loss in lift was about 15 percent and the loss in $C_{m\alpha}$ was approximately 25 percent (the loss in $C_{m\alpha}$ is relative to a pitching axis at 14.6 percent MAC).

Calculated $C_{L\alpha}$ values are shown as determined by reference 5 for an isolated 60° wing. Also shown are calculated wing-body $C_{L\alpha}$ values as determined by reference 6. The agreement between calculated values and the corrected experimental values is very good.

The aerodynamic-center position is shown in figure 9(a) against Mach number and was approximately constant over the test range at about 46 percent MAC. With aeroelasticity corrections as shown, the aerodynamic center moved rearward; at $M = 1.60$ this change in the aerodynamic-center position was about 4 percent MAC.

Shown in figure 9(b) are the damping-in-pitch derivatives ($C_{m_q} + C_{m_a}$) against Mach number. The sum of the derivatives varied from -1.6 to -1.2 for corresponding Mach numbers of $M = 1.28$ and $M = 1.60$. Calculated damping-in-pitch derivatives determined by reference 7 are also shown; the excellent agreement with the measured values would appear fortuitous. Damping-in-pitch derivatives from tunnel measurements, reference 8, are also in agreement with the present test.

CONCLUSIONS

The results of the present investigation of a 60° delta-wing-body configuration with an NACA 0003-63 airfoil section indicate the following conclusions for a Mach number range between $M = 1.28$ to $M = 1.60$:

1. The drag-due-to-lift parameter increased from 0.31 to 0.38 with increasing Mach number, and only a small amount of leading-edge suction was obtained.
2. C_L and C_m values varied linearly with α and the aerodynamic-center position was nearly constant at approximately 46 percent MAC.
3. The damping-in-pitch derivatives varied from -1.6 to -1.2 with increasing Mach number.
4. Values of $(L/D)_{max}$ decreased from 6.6 to 5.8; however, $C_{L_{opt}}$ remained nearly constant at 0.24 over the Mach number range.
5. Aeroelasticity effects calculated for the tested configuration increased with increasing Mach numbers and indicated a loss in lift of about 15 percent and a forward movement of the aerodynamic center of approximately 4 percent MAC at $M = 1.6$.

Langley Aeronautical Laboratory,
National Advisory Committee for Aeronautics,
Langley Field, Va., July 8, 1955.

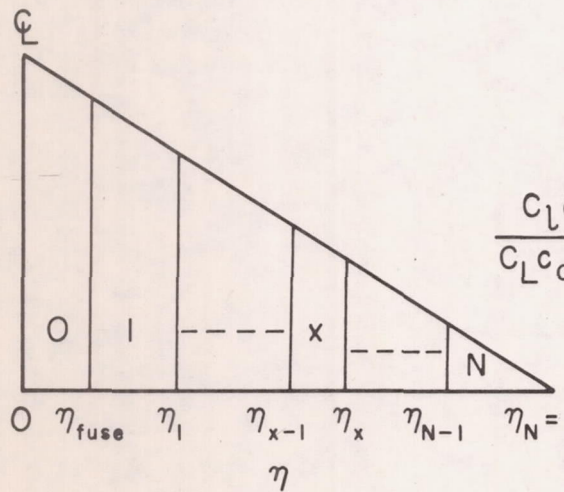
APPENDIX

AEROELASTICITY CORRECTIONS

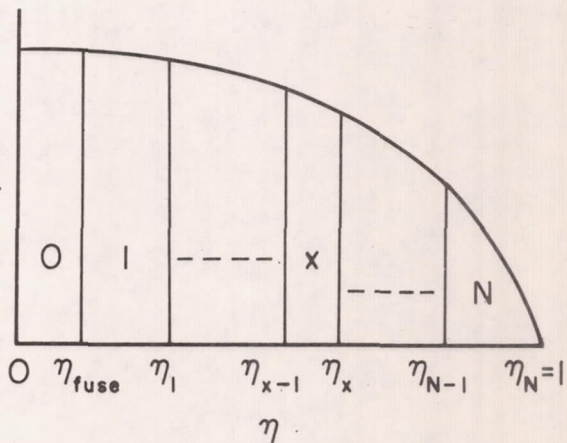
Aeroelasticity corrections to the wing-body lift and static longitudinal stability data have been made as was similarly made for exposed swept wings in reference 8. The derivation for flexibility effects for the wing-body configuration is presented as it is slightly different than when only the exposed wing panel is considered and in turn results in immediate wing-body flexibility effects.

The basic assumptions made in making the present corrections are: (1) the spanwise loading of the rigid wing mounted on the body is the same as for the isolated wing, that is, the body effects are negligible, (2) that the loaded flexible wing has a straight chord line at any spanwise station, (3) that in determining the structural influence coefficients, applying the loading along the approximate center of pressure chordline of the wing will result in coefficients representative of the loading in flight, and (4) aerodynamic induction effects are considered negligible after the initial rigid-wing loading.

The method requires both the rigid-wing spanwise loading curve and structural influence coefficients, and is essentially a form of strip theory in that the wing and its corresponding loading curve is divided into a series of strips (may be of varying widths) similar to the sketches below, where the (0) strip corresponds to the portion of the semispan within the fuselage.



$$\frac{C_L c}{C_L c_{av.}}$$



Spanwise Wing Loading

From the previous assumptions it is apparent that the lift of each strip of the flexible wing is directly proportional to $(\alpha_r + \Delta\alpha)$ where α_r is the angle of attack at the center line of the configuration or α for rigid-wing conditions, and $\Delta\alpha$ due to flexibility is the incremental α at the center of pressure of the strip. As the equilibrium $\Delta\alpha$ for any strip is dependent on the twisting of the other strips, the resulting lift on a strip will be given by the solution of a series of equations equal in number to the N number of strips into which the wing is divided.

The total lift over the semispan of a rigid wing is given as $L = C_{L\alpha_r} \alpha_r q S/2$, where α is in radians and the subscript r refers to center line or rigid conditions. Hence, the lift associated with any X -strip of the flexible wing would be given by

$$L_X = C_{L\alpha_r} q (S/2) K_X (\alpha_r + \Delta\alpha_X)$$

where (from the loading curve)

$$K_X = \int_{\eta_{X-1}}^{\eta_X} \frac{C_l c}{C_L c_{av}} d\eta$$

By dividing the expression for L_X by α_r an expression for $\frac{\Delta\alpha_X}{\alpha_r}$ is obtained

$$\frac{\Delta\alpha_X}{\alpha_r} = \frac{L_X}{\alpha_r} \frac{1}{C_{L\alpha_r} q (S/2) K_X} - 1$$

and to simplify for computational purposes

$$\frac{\Delta\alpha_X}{\alpha_r} = \frac{L_X}{\alpha_r} \frac{1}{Q K'_X} - 1 \quad (1)$$

where

$$Q = C_{L\alpha_r} q$$

$$K'_X = K_X S/2$$

the number of equations resulting being equal to the N number of strips chosen.

The incremental α due to flexibility can also be written in terms of the structural influence coefficients and for the $\Delta\alpha$ associated with the typical X-strip is,

$$\frac{\Delta\alpha_X}{\alpha_r} = \frac{L_1}{\alpha_r} \theta_{X1} + \frac{L_2}{\alpha_r} \theta_{X2} + \dots + \frac{L_X}{\alpha_r} \theta_{XX} + \dots + \frac{L_N}{\alpha_r} \theta_{XN} \quad (2)$$

where the general influence coefficient θ_{ij} is defined as the twist per unit load at the center of pressure of the strip i due to a load at the center of pressure of strip j . Again the number of equations resulting is equal to the N number of strips chosen.

Combining equations (1) and (2) and their corresponding expressions, yields the following set of equations:

$$\frac{L_0}{\alpha_r} = QK'{}_0$$

corresponding to the strip within the fuselage as indicated in the previous sketches, and then the $N-1$ simultaneous equations:

$$\frac{L_1}{\alpha_r} \left(\theta_{11} - \frac{1}{K'{}_1 Q} \right) + \frac{L_2}{\alpha_r} \theta_{12} + \dots + \frac{L_X}{\alpha_r} \theta_{1X} + \dots + \frac{L_N}{\alpha_r} \theta_{1N} = -1$$

.

$$\frac{L_1}{\alpha_r} \theta_{X1} + \frac{L_2}{\alpha_r} \theta_{X2} + \dots + \frac{L_X}{\alpha_r} \left(\theta_{XX} - \frac{1}{QK'{}_X} \right) + \dots + \frac{L_N}{\alpha_r} \theta_{XN} = -1$$

.

$$\frac{L_1}{\alpha_r} \theta_{N1} + \frac{L_2}{\alpha_r} \theta_{N2} + \dots + \frac{L_X}{\alpha_r} \theta_{XN} + \dots + \frac{L_N}{\alpha_r} \left(\theta_{NN} - \frac{1}{QK'{}_N} \right) = -1$$

.

The above equations are solved for $\frac{L_0}{\alpha_r}$, $\frac{L_1}{\alpha_r}$, $\frac{L_2}{\alpha_r}$, \dots , $\frac{L_X}{\alpha_r}$, \dots , $\frac{L_N}{\alpha_r}$ in terms of specific values of Q (the values are chosen corresponding to the test range). With the solution of the previous equations the following expression can be written,

$$\left(\frac{C_{L\alpha_f}}{C_{L\alpha_r}} \right) = \frac{\frac{L_0}{\alpha_r} + \frac{L_1}{\alpha_r} + \dots + \frac{L_X}{\alpha_r} + \dots + \frac{L_N}{\alpha_r}}{QS/2}$$

which is the ratio of the lift of the flexible-wing configuration to that of a rigid-wing configuration. $C_{L_{ar}}$ can be determined from a plot of the above expression for the assumed specific values of Q previously referred to, for any given q value and in turn its corresponding Mach number.

The spanwise center of pressure for the flexible wing is given by

$$(y_{CP})_f = \frac{\frac{L_0}{\alpha_r} y_0 + \frac{L_1}{\alpha_r} y_1 + \dots + \frac{L_X}{\alpha_r} y_X + \dots + \frac{L_N}{\alpha_r} y_N}{\frac{L_0}{\alpha_r} + \frac{L_1}{\alpha_r} + \dots + \frac{L_X}{\alpha_r} + \dots + \frac{L_N}{\alpha_r}}$$

hence

$$\Delta \frac{\partial C_m}{\partial C_L} = \frac{[(y_{CP})_r - (y_{CP})_f]}{\bar{c}} \tan \Lambda$$

where Λ is the approximate sweep of the center-of-pressure chord line.

And finally $C_{m_{ar}}$ is given by $C_{m_{ar}} = C_{L_{ar}} \left(\frac{\partial C_m}{\partial C_L} \right)_r$.

As previously mentioned, the method requires a linear chordwise variation of the flexible-wing chord plane at any spanwise station; hence, it seemed questionable that it could be used for delta wings in general. However, in finding the experimental influence coefficients, it was found that with a spanwise loading along the 46 percent chord line (representative of 60° delta wings in this speed range) resulted in a linear variation for this wing within the accuracy of the measurements. The final justification of assuming a linear chordwise variation is in the agreement of the corrected lift values with those measured under near rigid-wing conditions.

For the present test, the wing was divided into six strips which, from previous tests, seemed to be an adequate number. Though inertia effects can easily be included in the present method, a rough check indicated the inertia effects of the present wing were negligible; hence, no corrections for these effects were included.

REFERENCES

1. Osborne, Robert S., and Kelly, Thomas C.: A Note on the Drag Due to Lift of Delta Wings at Mach Numbers Up to 2.0. NACA RM L53A16a, 1953.
2. Gillis, Clarence L., Peck, Robert F., and Vitale, A. James: Preliminary Results From a Free-Flight Investigation at Transonic and Supersonic Speeds of the Longitudinal Stability and Control Characteristics of Airplane Configurations with a Thin Straight Wing of Aspect Ratio 3. NACA RM L9K25a, 1950.
3. Vitale, A. James: Effects of Wing Elasticity on the Aerodynamic Characteristics of an Airplane Configuration Having 45° Sweptback Wings as Obtained from Free-Flight Rocket-Model Tests at Transonic Speeds. NACA RM L52L30, 1953.
4. Hall, Charles F.: Lift, Drag, and Pitching Moment of Low-Aspect Ratio Wings at Subsonic and Supersonic Speeds. NACA RM A53A30, 1953.
5. Brown, Clinton E.: Theoretical Lift and Drag of Thin Triangular Wing at Supersonic Speeds. NACA Rep. 839, 1946. (Supersedes NACA TN 1183.)
6. Neilson, Jack N., Katzen, Elliott D, and Tang, Kenneth K.: Lift and Pitching-Moment Interference Between a Pointed Cylindrical Body and Triangular Wings of Various Aspect Ratios at Mach Numbers of 1.50 and 2.02. NACA RM A50F06, 1950.
7. Henderson, Arthur, Jr.: Pitching-Moment Derivatives C_{m_q} and C_{m_d} at Supersonic Speeds for a Slender-Delta-Wing and Slender-Body Combination and Approximate Solutions for Broad-Delta-Wing and Slender-Body Combinations. NACA TN 2553, 1951.
8. Tobak, Murray: Damping in Pitch of Low-Aspect-Ratio Wings at Subsonic and Supersonic Speeds. NACA RM A52L04a, 1953.

TABLE I

FUSELAGE ORDINATES

Distance from nose of fuselage, in.	Fuselage radius, in.
0	0
.390	.097
.585	.145
.975	.239
1.950	.469
3.900	.902
5.850	1.298
7.800	1.658
11.700	2.267
15.600	2.730
19.500	3.047
23.400	3.218
27.300	3.248
31.200	3.221
35.100	3.161
39.000	3.069
42.900	2.943
46.800	2.785
50.700	2.594
54.600	2.371
58.500	2.115
62.400	1.826
65.000	1.615

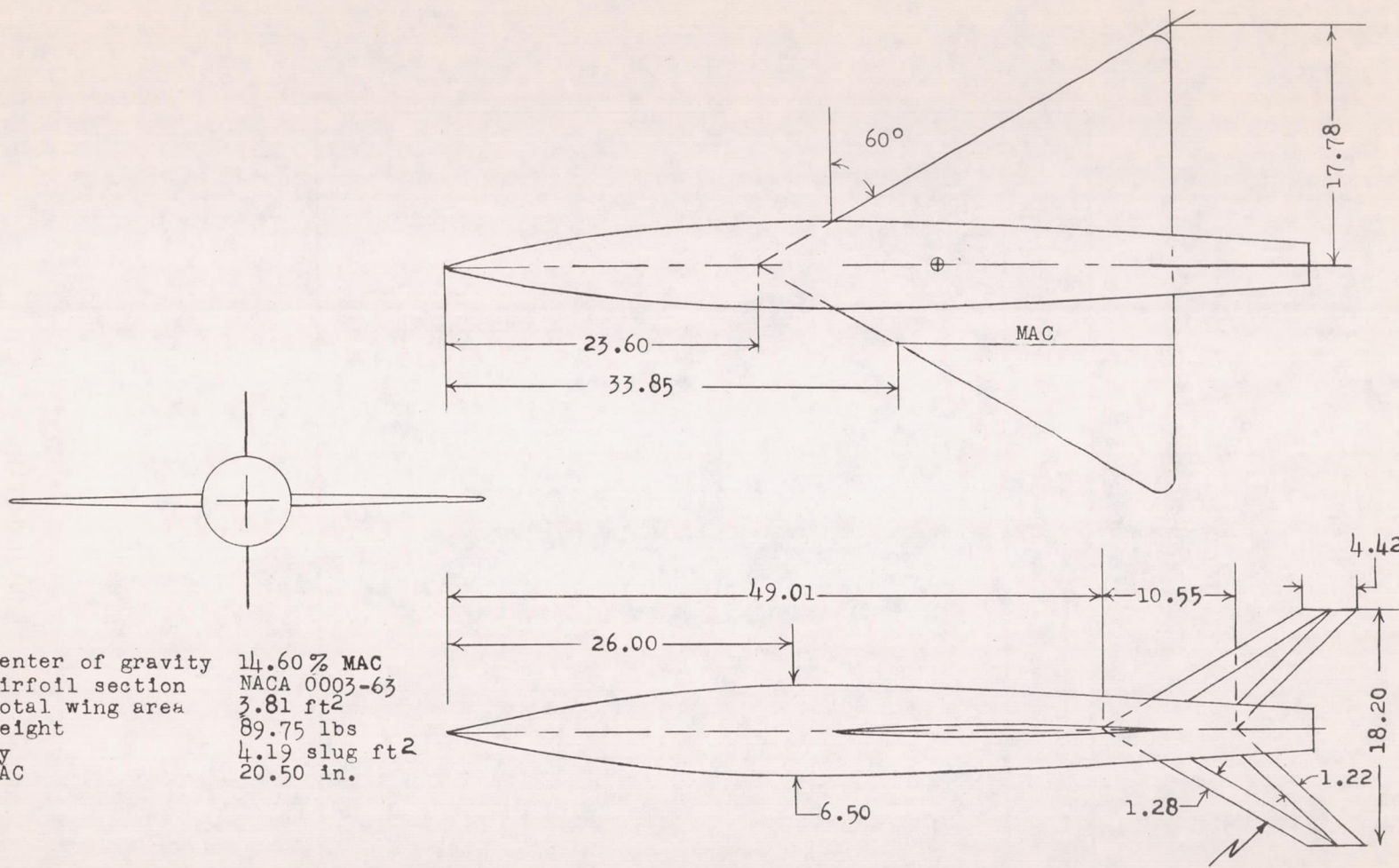
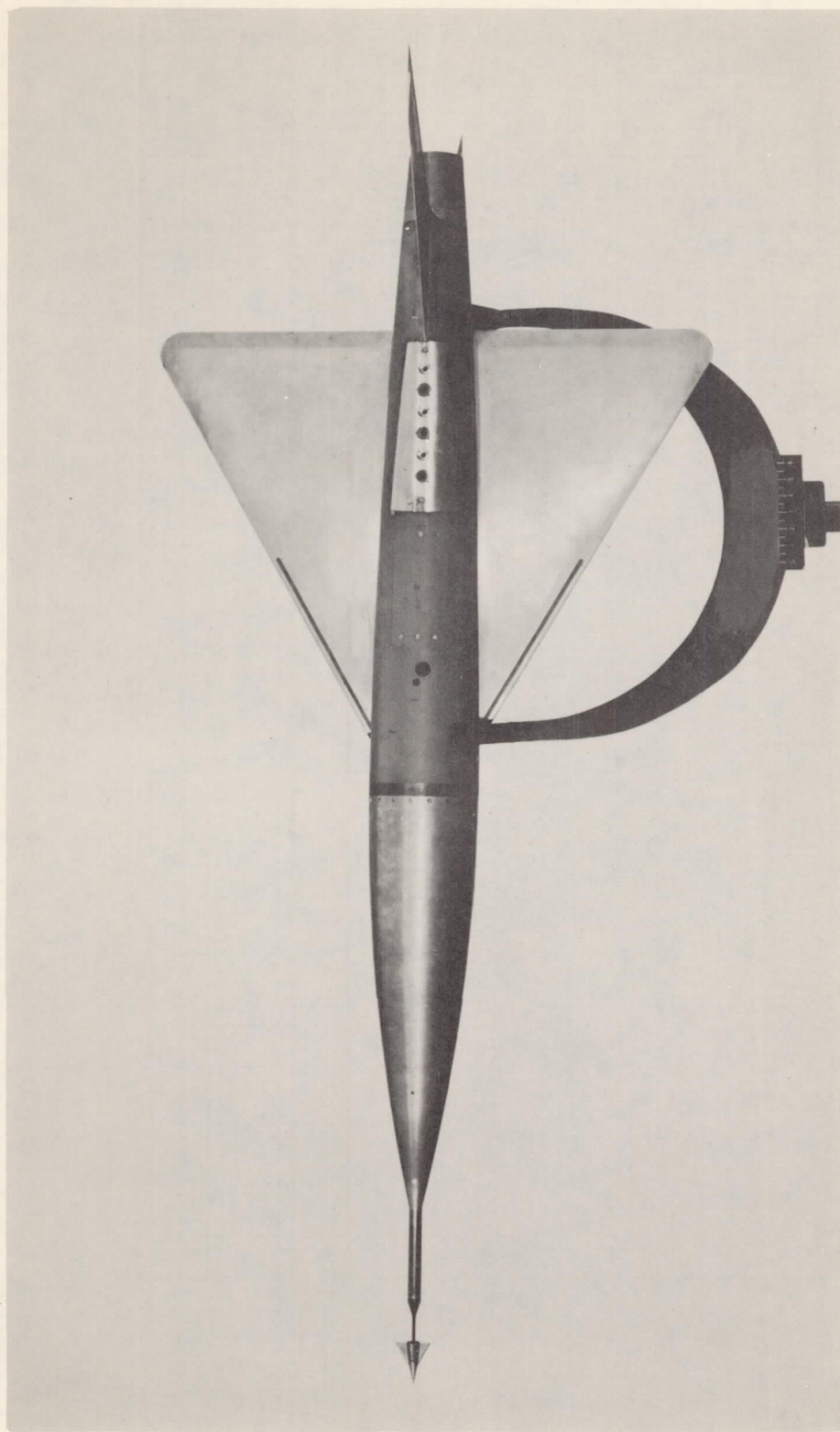


Figure 1.- Sketch of the tested configuration, all linear dimensions in inches.



L-85786.1

Figure 2.- Photograph of the tested configuration.

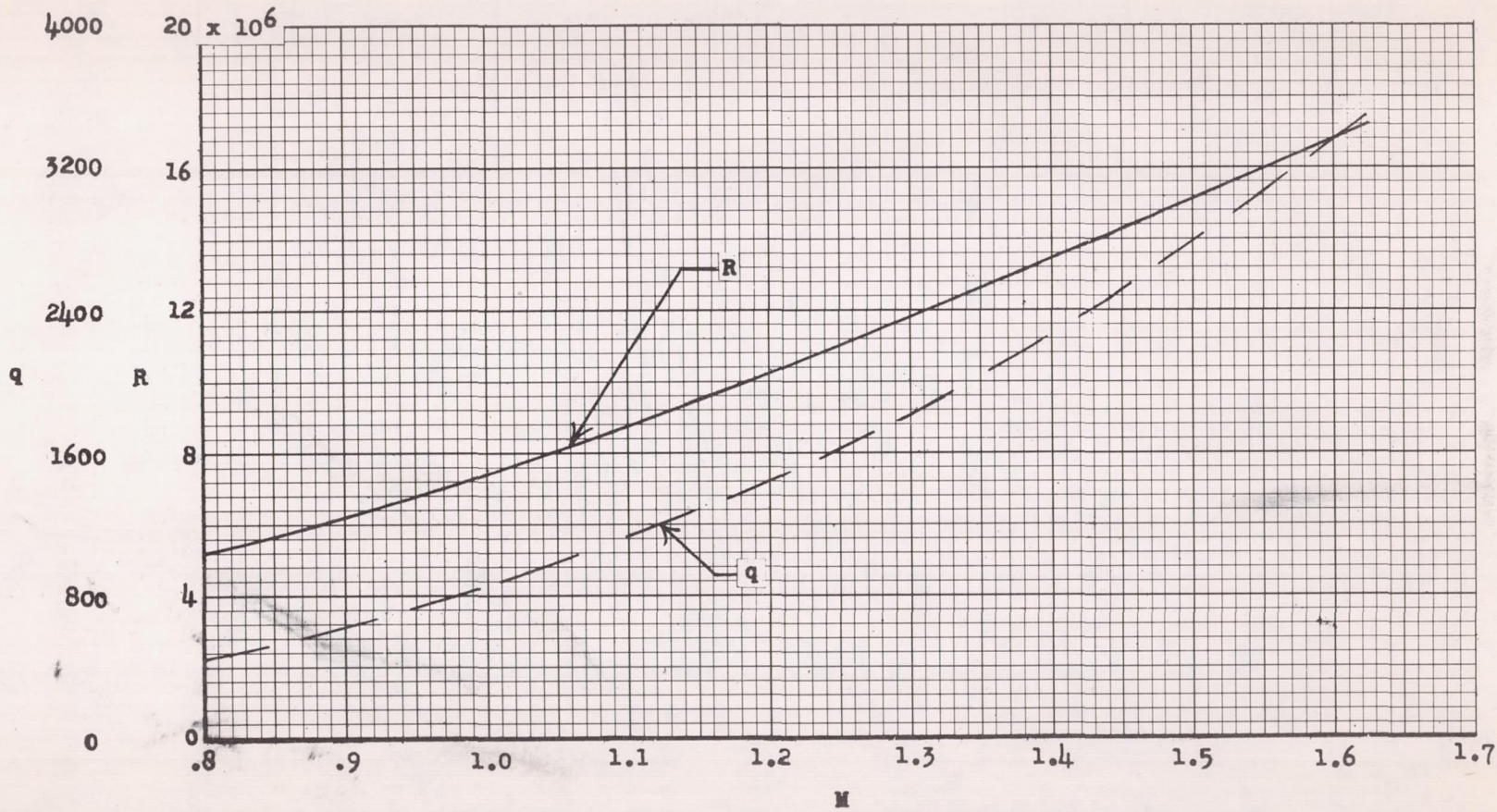


Figure 3.- Variations of Reynolds number based on mean aerodynamic chord and q with Mach number.

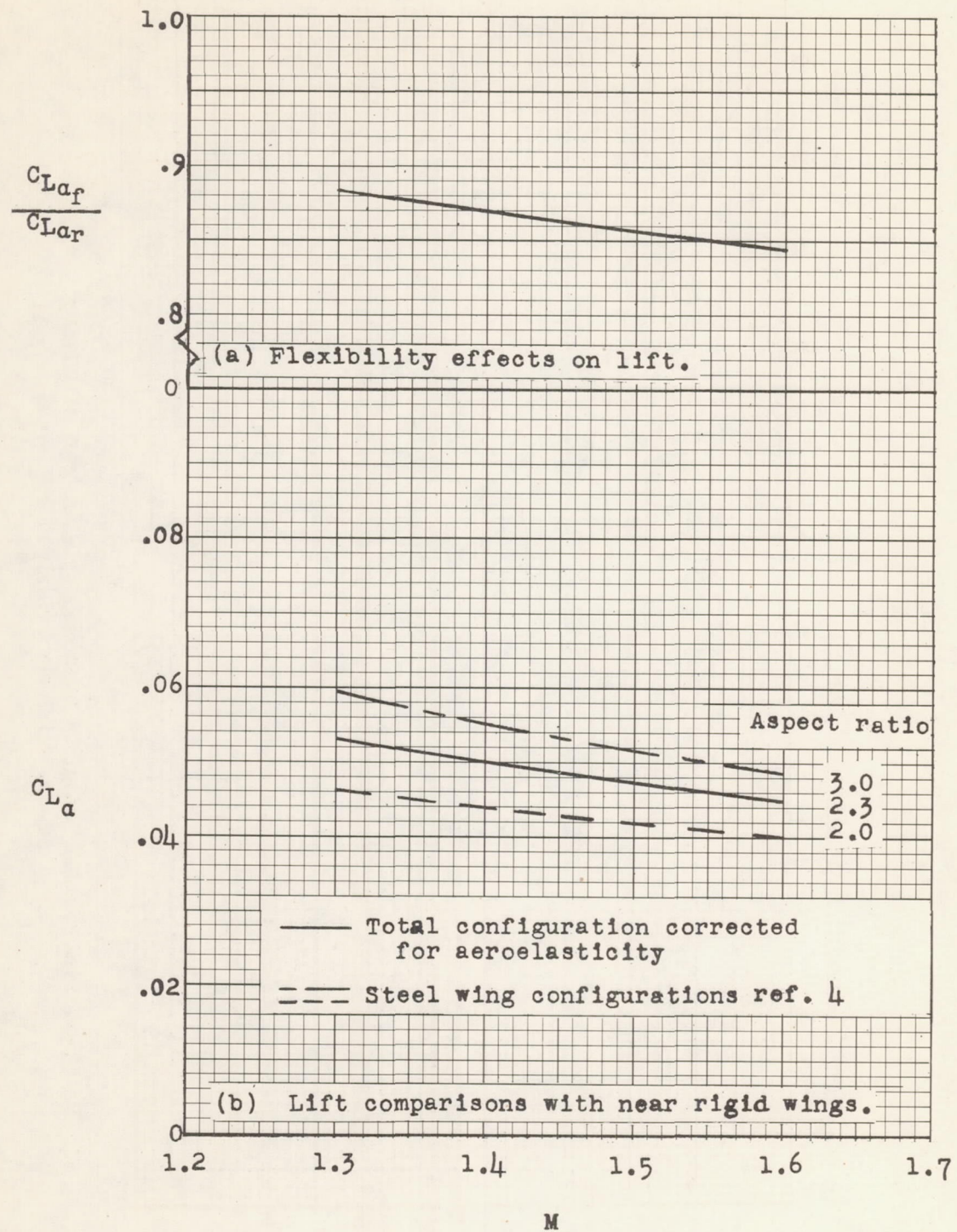


Figure 4-- Lift characteristics of the tested configuration and comparisons with near rigid wings.

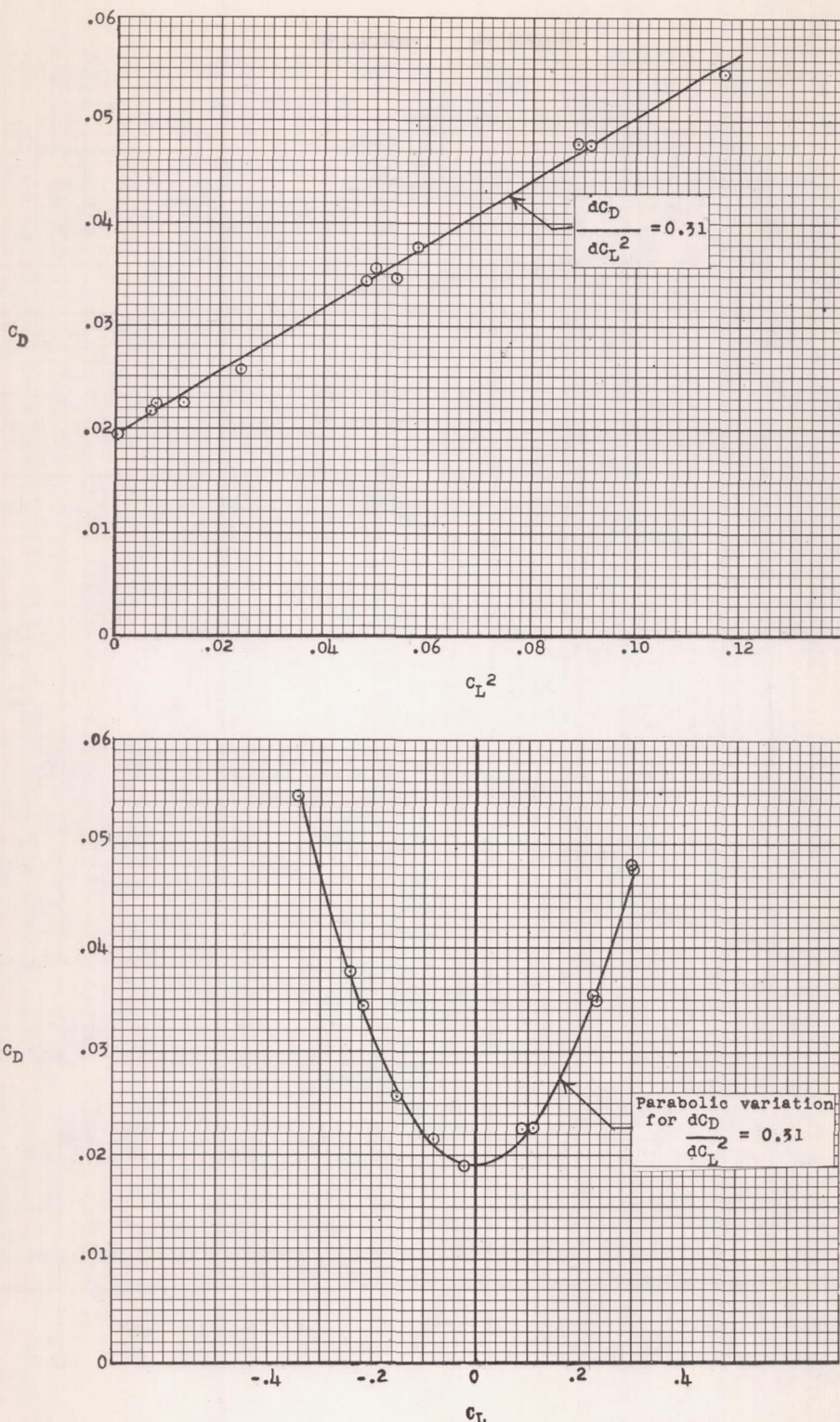


Figure 5.- Typical C_D curves showing actual test points. (First cycle of $M = 1.3$ oscillation.)

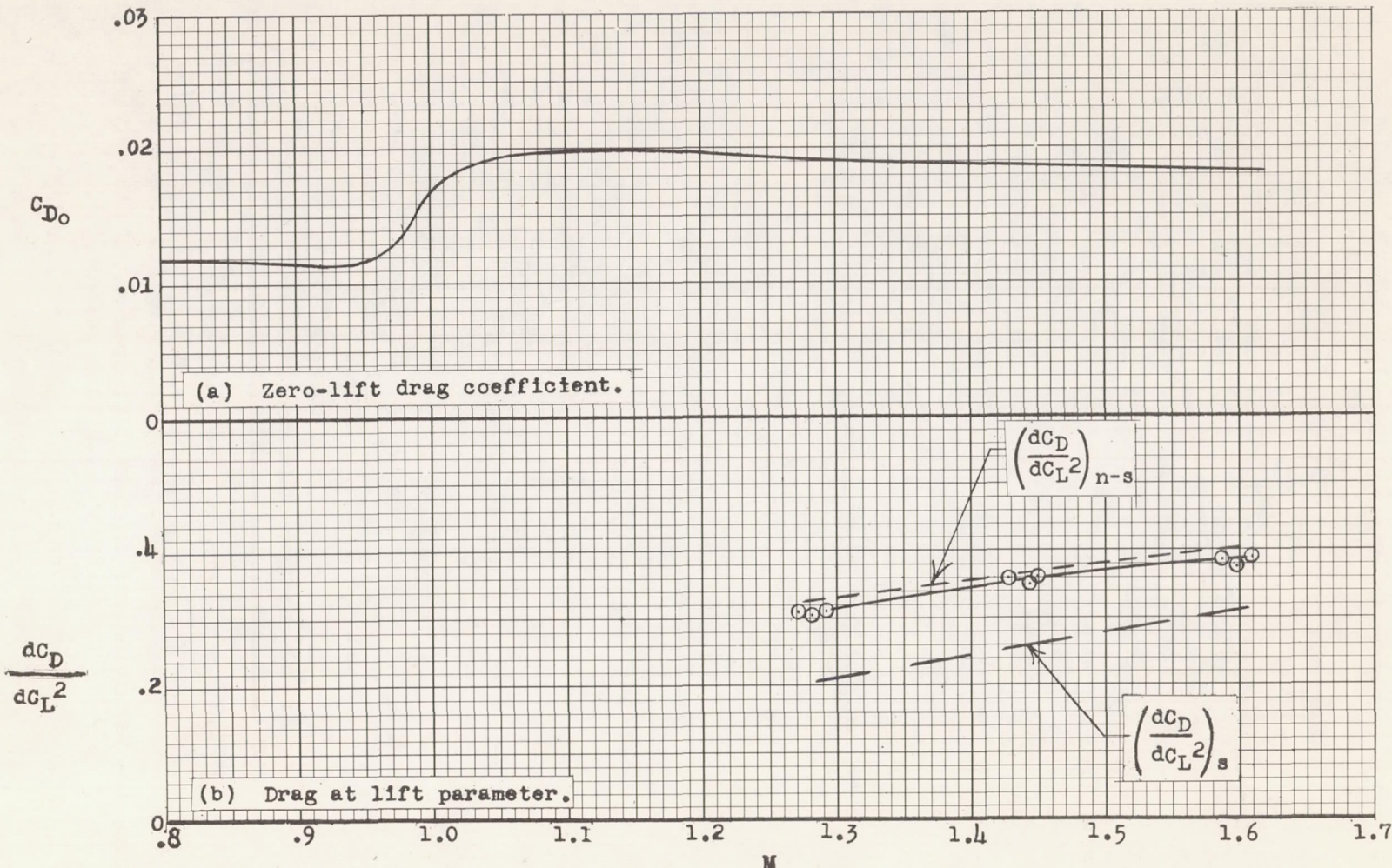


Figure 6.- Variations of zero-lift drag and drag at lift with Mach number.

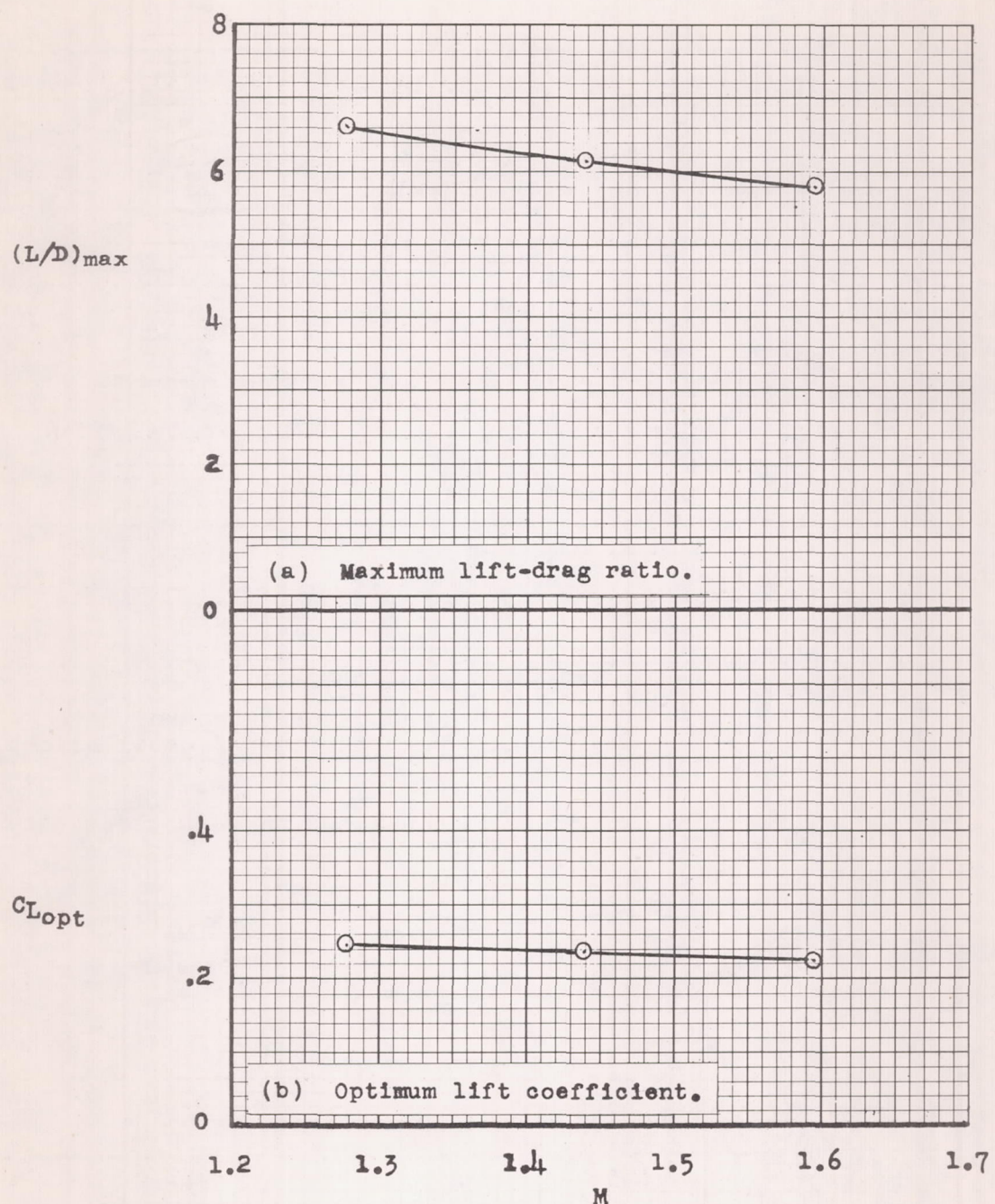


Figure 7.- Variations of maximum lift-drag ratio and optimum lift coefficient with Mach number.

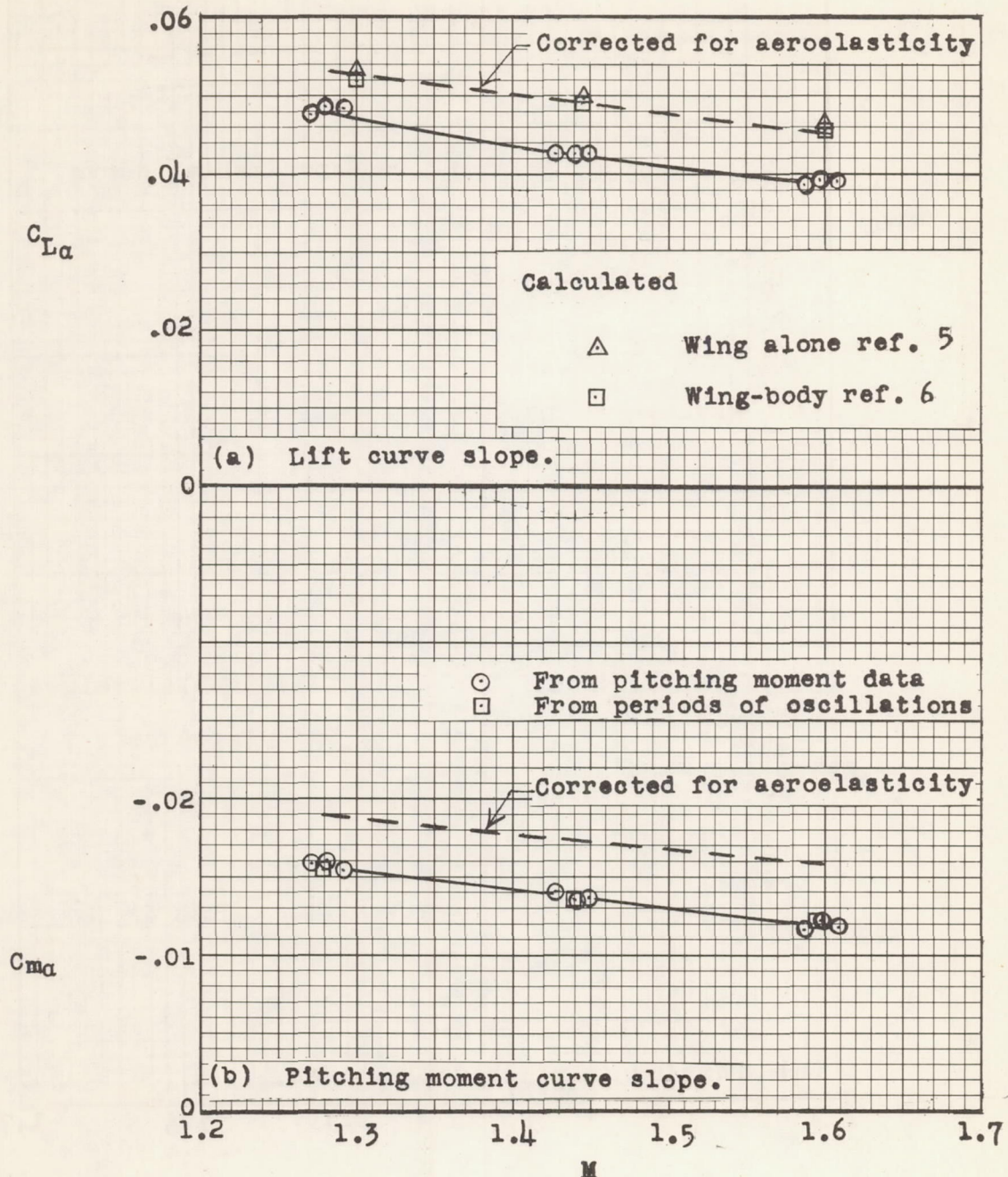


Figure 8.- Variations of the slopes of the lift and moment curves with Mach number including aeroelasticity corrections.

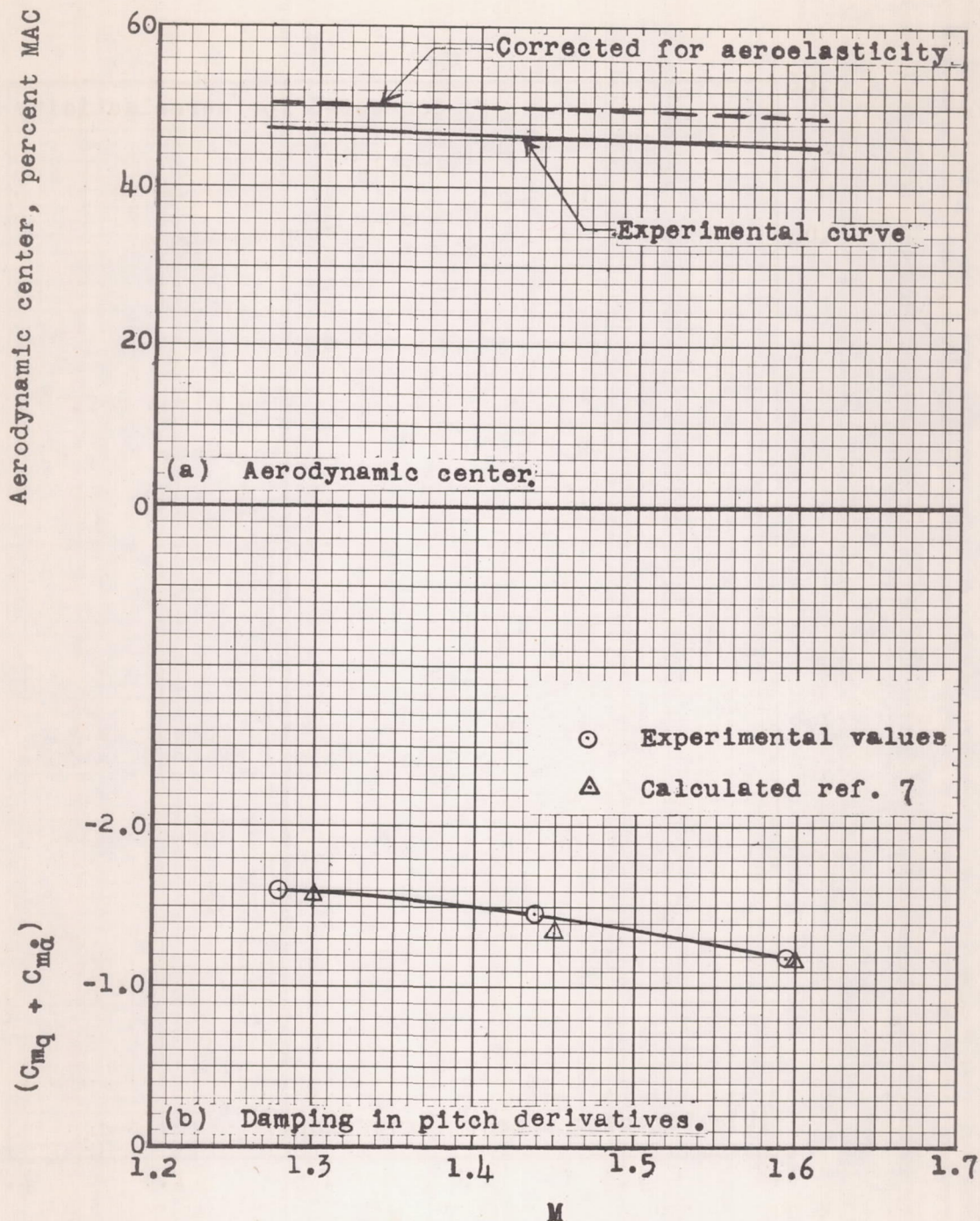


Figure 9.- Variations of the aerodynamic center and damping in pitch derivatives with Mach number.

CONFIDENTIAL

CONFIDENTIAL